

Effect of Long-Time Postweld Heat Treatments on the Mechanical Properties of a Carbon-Manganese Pressure Vessel Steel

G. Pimenta and F. Bastian

(Submitted 21 April 2000; in revised form 8 November 2000)

Postweld heat treatment is a common practice among building codes for welded steel structures and equipment to reduce the high as-welded residual stress level, improve the fracture toughness, and increase the critical size of acceptable defects. There are many discrepancies among international building codes for storage spheres, pressure vessels, and welded structure components about parameters such as duration and temperature for postweld heat treatments. Furthermore, the codes frequently omit the top number of thermal cycles, which the structure may support to maintain the mechanical properties and toughness in an acceptable level, keeping the physical integrity of the equipment. The present work analyzes the effect of duration of the postweld heat treatments on the mechanical properties and fracture toughness of a carbon-manganese steel of specification ASTM A-516 G 70, which frequently is used to build spheres and pressure vessels in the petrochemical industry. The regions corresponding to the base metal (BM) and heat-affected zone (HAZ) were studied. Through the results obtained from the tensile tests, hardness measurements, Charpy V-notch impact and crack-tip opening displacement (CTOD) testing, and microstructural characterization, it is concluded that the mechanical properties and fracture toughness were reduced by increasing the time of the postweld heat treatment. The degradation of the original properties of the steel is attributed to the changes that occurred in the microstructure. With the welding procedure used, it was verified that the fracture resistance of the HAZ was higher than that of the BM.

Keywords mechanical properties, postweld heat treatments, pressure vessel steels

1. Introduction

Pressure vessels and spheres for storage of liquid petroleum gas (LPG), propane, and butane are susceptible to the occurrence of cracks in the welded joints during their service lifes.

Data published recently[1] have shown that the cracks in the welds and heat-affected zones (HAZs) of the joints can have sizes as large as 25 mm length and 3 mm depth to 1000 mm length and 12 mm depth.

The origin of those cracks is mainly due to two factors:

- fabrication defects, during the welding operation; and
- cracks nucleated and/or propagated during the operation of the equipment, mainly when the fluid stored is contaminated with water and hydrogen sulfide (H_2S).

Two classes of steels are normally used for the fabrication of storage spheres and pressure vessels:

- high strength steels, with an ultimate tensile strength (UTS) higher than 480 MPa (70 ksi), allowing the use of relatively thin plates, which do not necessitate stress relief heat treatments. (these materials require, on the other hand, very careful and controlled welding procedures and present high risk of hydrogen cracking); and
- low strength steels, with an UTS lower than 480 MPa, which require thicker plates and, consequently, postweld stress relief heat treatments.

G. Pimenta, PETROBRAS-CENPES, Quadra 7, Ilha do Fundão, 21949-900, Rio de Janeiro, RJ, Brazil; and **F. Bastian,** COPPE/UFRJ, Metallurgical and Materials Engineering, Caixa Postal 68505, Rio de Janeiro, 21945-970 Brazil. Contact e-mail: fbastian@metalmat.ufrj.br.

Around the world nowadays there are several spheres with a relatively high number of cracks. Most of these spheres were fabricated using steels of the specification ASTM A-516 G 70 and fabricated following the Code ASME Section VIII, Divisions 1 and 2.[2] Some of these spheres were already subjected to more than two heat treatments, which follow the repair of the defects, sometimes above that allowed by the standard.

The stress relief heat treatment is a practice that is common among the standards of construction of welded steel structures due to three main reasons:

- to reduce the residual stresses along and through the welds;
- to improve the mechanical properties of the welded joints, mainly the fracture toughness; and
- to increase the size of acceptable defects.

There are several disparities among the international standards in relation to the specification of the thermal cycle in stress relief heat treatments for carbon-manganese and microalloyed steels, such that all of them are omitting in relation to the number of thermal cycles that is possible to submit the structure while keeping their mechanical properties at acceptable levels.

The objective of the present work is to study the effect of

Table 1 Chemical composition of the steel studied

Element	Chemical composition (wt.%)							
	C	Si	Mn	Al	Ni	Ti	S	P
Wt.%	0.25	0.24	1.00	0.05	0.07	0.01	0.015	0.018

Table 2 Welding parameters

Electrode	E-7018
Joint geometry	Type K
Polarity	Inverse
Type of current	Continuous
Welding speed	10 to 18 cm/min
Welding position	1 G
Interpass temperature	250 °C (maximum)
Preheating temperature	125 °C (minimum)
Electrode diameter	
Root	3.25 mm
Filler	4.00 mm
Welding current	
Root	75–120 A
Filler	120–225 A
Arc voltage	
Root	20–25 V
Filler	22–27 V

the time of the heat treatment of stress relief on the tensile properties, hardness, and fracture resistance of the base metal (BM) and HAZ of a welded joint of a steel of the specification ASTM A-516 Gr 70.[3] The temperature chosen for the heat treatment was 620 °C, and the times of the heat treatments were 2.3, 6.3, 14.0, and 21.2 h, corresponding to 1, 3, 6, and 10 treatments, respectively.

The fracture resistance of the material was evaluated through Charpy-V-notch impact tests and the crack-tip opening displacement (CTOD) testing method. A microstructural characterization using optical and scanning electron microscopy was performed, and a fractographic analysis of the broken Charpy testpieces was also performed using scanning electron microscopy.

2. Materials

2.1 Steel Studied

A plate of steel ASTM A-516 G 70 of 65 mm thickness was used in the work. The chemical composition of the steel is presented in Table 1.

2.2 Welding Procedure

For the study, welded joints of type K were used in order to produce a uniform HAZ parallel to the flat side of the joint.

The welding procedure followed the standard ASME/AWS.[4] The welding parameters and the details of the preparation of the joint are presented in Table 2 and Fig. 1.

Strips of 300 mm width were cut parallel to the rolling direction of the plates and welded in pairs along the cut edges. The welding operation was performed by welders qualified following the ASME standard. The welded joints were inspected using penetrant liquid in the root pass, in both sides of the joint, and visual inspection of the filling passes, after cleaning. After the welding operation, the welded joints were inspected by gammagraphy. Regions with defects were also inspected by ultrasound, and, depending on the defect, they were discharged.

Table 3 Symbology

Time at 620 °C (h)	2.3	6.3	14.0	21.2
Symbol	T2.3	T6.3	T14.0	T21.2

2.3 Stress-Relief Heat Treatments

Strips of the BM and welded strips were heat treated in an electric resistance industrial furnace with programmable control of temperature.

The temperature of the treatment was 620 ±5 °C. The specimens were maintained at this temperature range for continuous time periods of 2.3, 6.3, 14.0, and 21.2 h, corresponding to 1, 3, 6, and 10 heat treatments, respectively.

The heating and cooling rates were as follows:

- heating rate: 220 °C/h in maximum (above 315 °C); and
- cooling rate: 260 °C/h in maximum (until 315 °C, and then cooling in air).

3. Experimental Methods

3.1 Testpieces

The testpieces were made from the heat-treated material following the relevant standards. In order to identify the different heat treatments, the symbology adopted is shown in Table 3.

3.2 Macrographic Examination

Two samples of 10 mm width and 100 mm length were cut from the heat-treated material for a macrographic examination and measurement of hardness. After polishing, the samples were etched with a Nital 2 solution in order to check for the uniformity of the weld groove and the HAZ.

3.3 Metallography

A metallographic analysis was performed in order to characterize the microstructures resulting from the different heat treatments. A Nital 2 solution was used to etch the samples. A

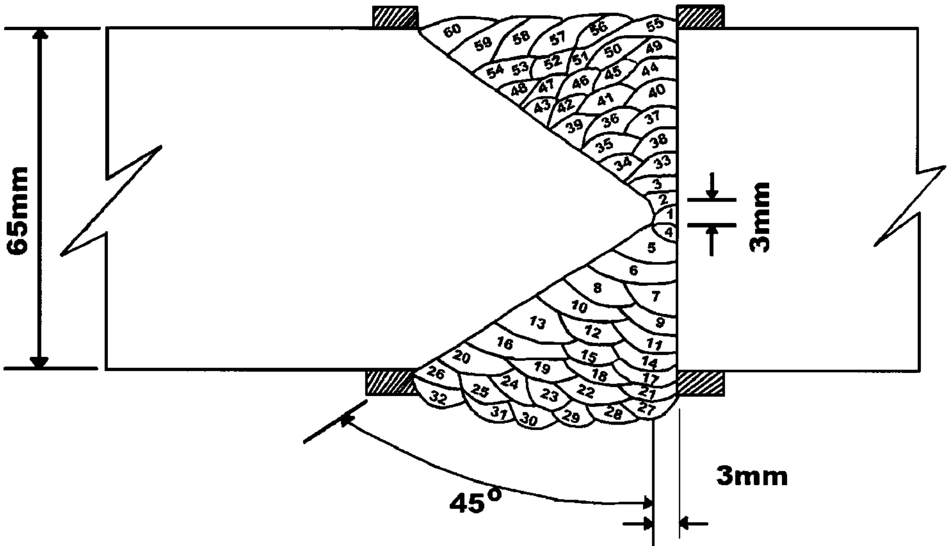

Fig. 1 Geometry of the welded joint and sequence of the welding passes

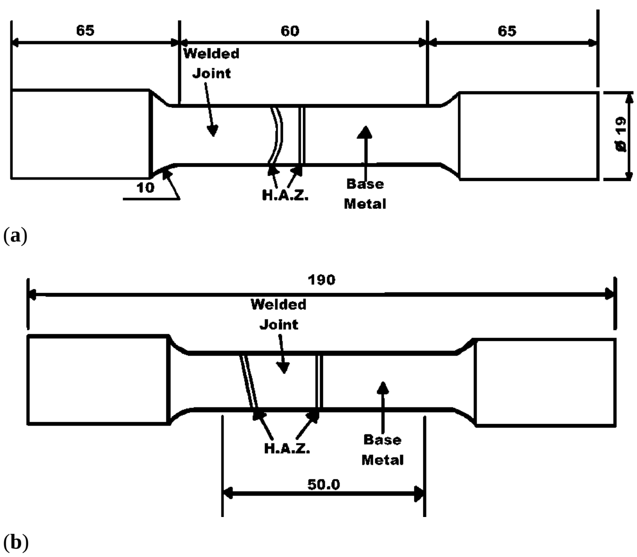

Fig. 2 Tensile testpieces of the welded joint. (**a**) Testpiece from the half-thickness region of the plate. (**b**) Testpiece from the surface of the plate. The dimensions of the testpieces from the BM are similar. Dimensions in millimeters

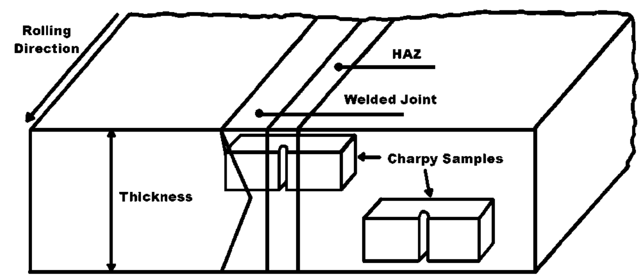

Fig. 3 Location of the Charpy testpieces

scanning electron microscope JEOL model JXA 8440A (Japan Electron Optics Ltd., Tokyo) was used for the observations.

3.4 Tensile Testing

The tensile tests were performed following the standard ASTM E 8M[5] in a screw driven Panambra model 100 TU2634 universal testing machine of 200 MN with an electronic extensometer.

The tensile testpieces had a circular section with the dimensions shown in Fig. 2. They were cut transversally to the rolling direction at half-thickness. Specimens from the BM and the welded joints were tested at room temperature. At least three specimens were tested for each heat-treated condition.

3.5 Hardness Measurements

The Rockwell A hardness[6] of the samples was measured at a distance of 5 mm from the surface of the plate, at half-thickness and along the HAZ. The macrographic samples were used for this purpose.

The Vickers microhardness[7] was also evaluated in the same regions of the measurements of Rockwell A hardness.

3.6 Charpy-V-Notch Impact Testing

The Charpy impact tests were performed following the standard E-23.[8] The notches were machined in the fusion line of the HAZ and in the BM, parallel to the rolling direction, as shown in Fig. 3, corresponding to the orientation T-L of the standard ASTM E616.[9]

The tests were performed at temperatures of 40, 23, 0, −10, −20, −40, and −60 °C. A mixture of liquid nitrogen and ethilic alcohol was used. Four testpieces were used for each temperature.

The samples taken from the welded joints were etched in a solution of Nital 2 to reveal the HAZ, allowing location of the machined notch.

A Tokyo impact testing machine model EC-30 was used.

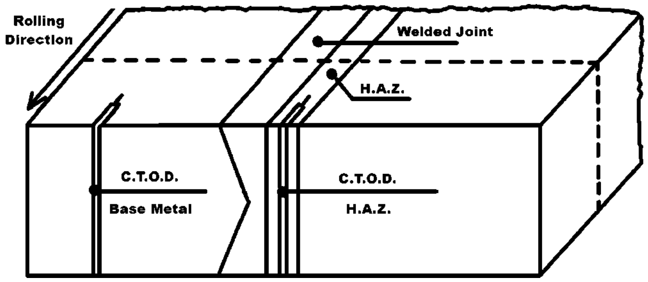

Fig. 4 Location of the CTOD testpieces

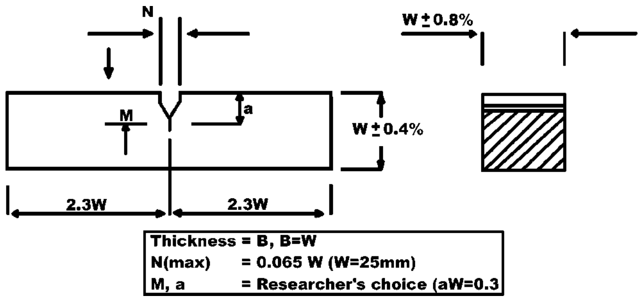

Fig. 5 Geometry and dimensions of the CTOD testpieces

3.7 CTOD Testing

The tests were performed following the standard BS5762/79.[10,11] The location of the CTOD testpieces in the joint is shown in Fig. 4.

The subsidiary testpiece was used with the fatigue precracks parallel to the rolling direction, corresponding to the orientation T-L of the standard ASTM E616,[9] as shown in Fig. 5.

The BM and the HAZ were tested. The tests were performed at 27, 0, −20, −30, −40, and −60 °C. A MTS (MTS Systems Co., Eden Prairie, MN) servohydraulic machine model 442 equipped with a load cell of 100 MN was used for the tests.

3.8 Fractography

A fractographic analysis of the Charpy testpieces with an absorbed impact energy at fracture of 20 J was performed using the JEOL scanning electron microscope above.

4. Experimental Results

4.1 Macrography

Prior to making the mechanical tests, a macrographic examination of sections taken from the welded joints was performed to check for the uniformity of the welds and HAZs. A macrographic examination was also performed to check if the notches of the Charpy and CTOD testpieces were correctly located in the HAZs. Figure 6 illustrates the different regions of the welded joint of the work.

4.2 Metallography

The heat treatment at the temperature of 620 °C for long times promoted a spheroidization and coalescence of the cementite lamella of the pearlite, as shown by Fig. 7, corresponding to the treatment of 2.3 h, and Fig. 8 corresponding to the treatment of 21.2 h.

A coalescence of the carbide particles of the HAZ also took place as a result of the increase of the holding time at the temperature of 620 °C. This is illustrated by Fig. 9 and 10 corresponding to 2.3 and 21.2 h of treatment, respectively.

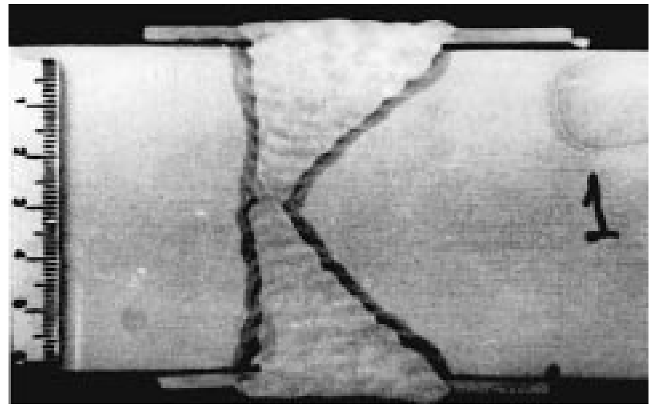

Fig. 6 Macrography of the welded joint. Etching with Nital 2

Fig. 7 Microstructure of the BM subjected to the heat treatment for 2.3 h. SEM

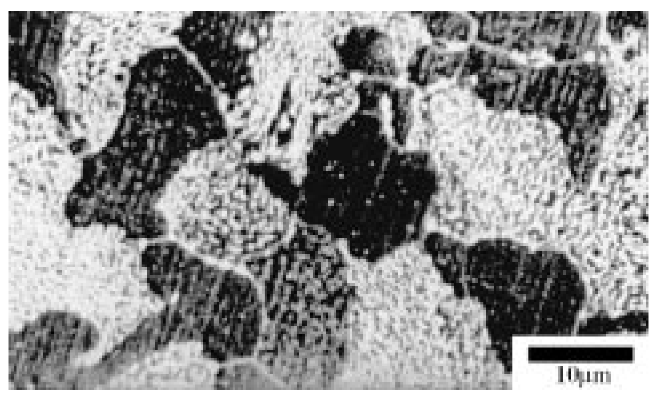

Fig. 8 Microstructure of the BM subjected to the heat treatment for 22.2 h. SEM

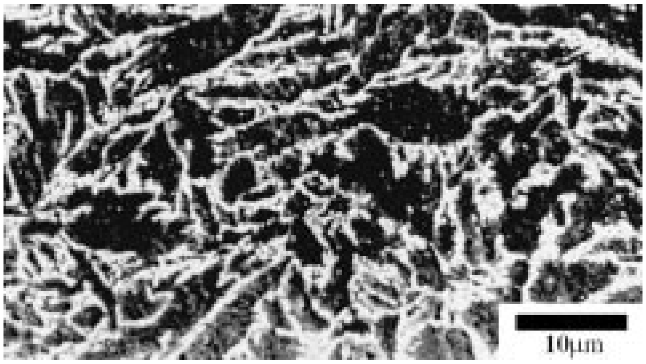

Fig. 9 Microstructure of the HAZ subjected to the heat treatment for 2.3 h. SEM

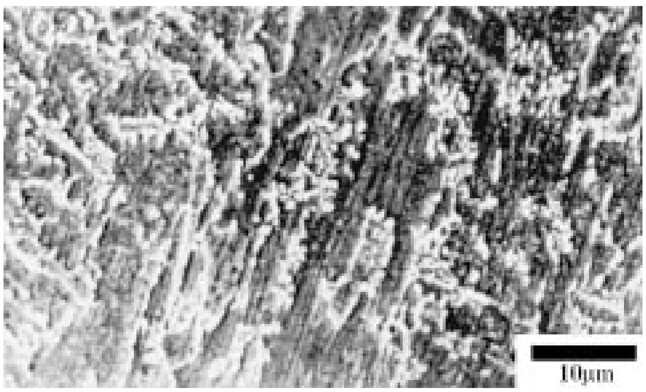

Fig. 10 Microstructure of the HAZ subjected to the heat treatment for 21.2 h. SEM

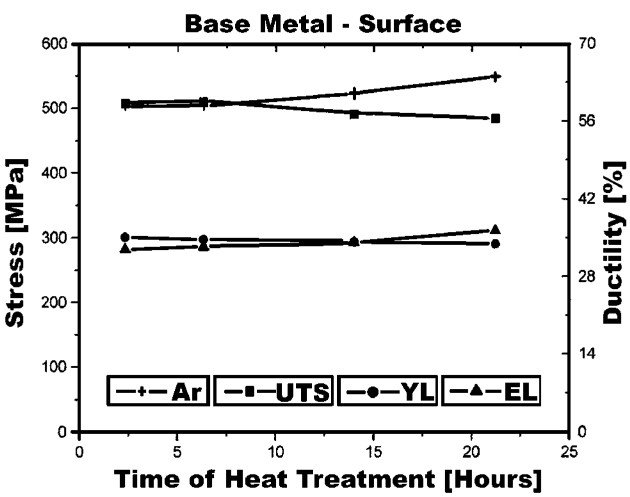

Fig. 11 Tensile properties of the BM (region of the surface of the plate) as a function of the time of treatment at 620 °C

4.3 Tensile Testing

The results of the tensile tests of the heat-treated material are shown in Fig. 11 to 14, where each point corresponds to the mean of three values.

The figures show that the yield limit (YL) and UTS of both

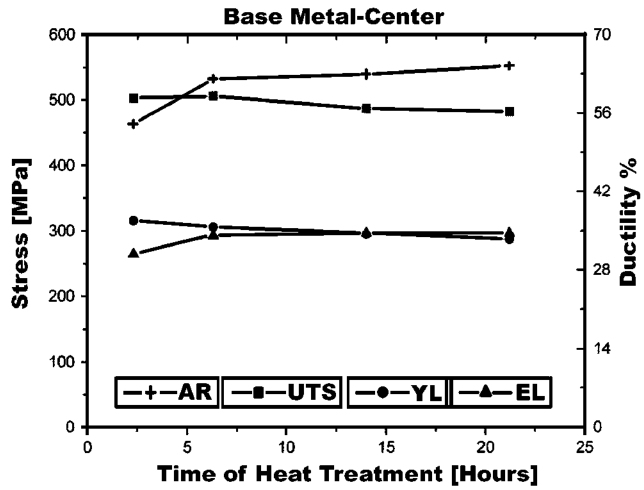

Fig. 12 Tensile properties of the BM (region of half-thickness of the plate) as a function of the time of treatment at 620 °C

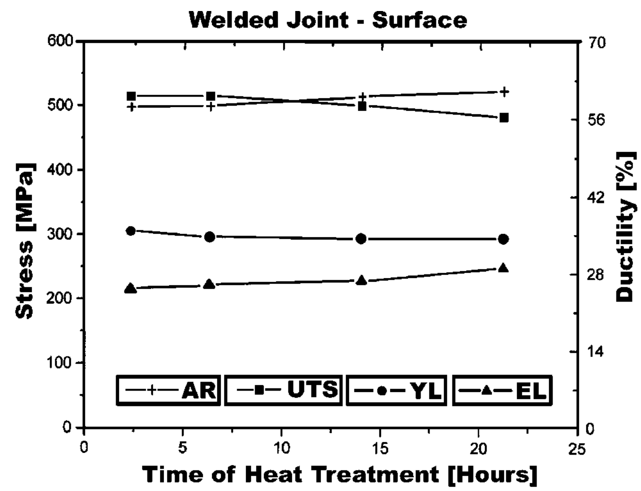

Fig. 13 Tensile properties of the HAZ (region of the surface of the plate) as a function of the time of treatment at 620 °C

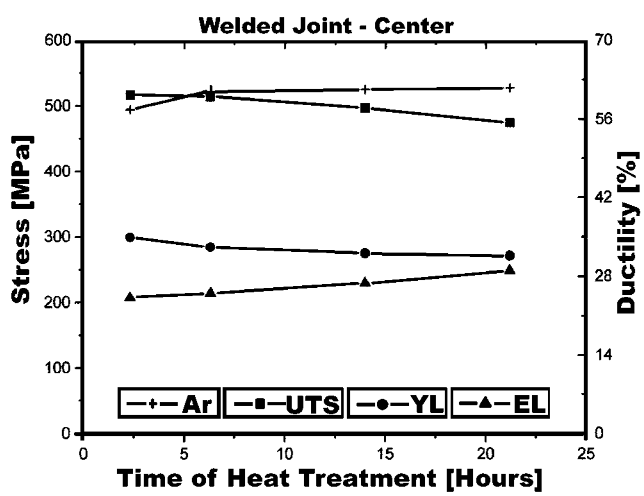

Fig. 14 Tensile properties of the HAZ (region of half-thickness of the plate) as a function of the time of treatment at 620 °C

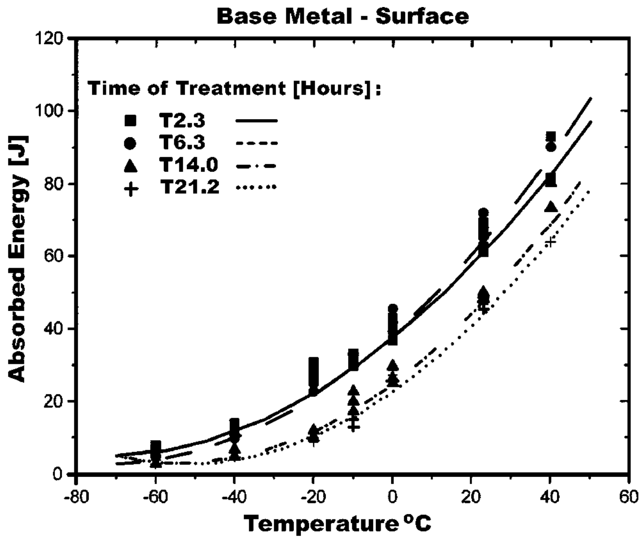

Fig. 15 Charpy absorbed impact energy of the BM (region of the surface), for the different heat treatments, as a function of the testing temperatures

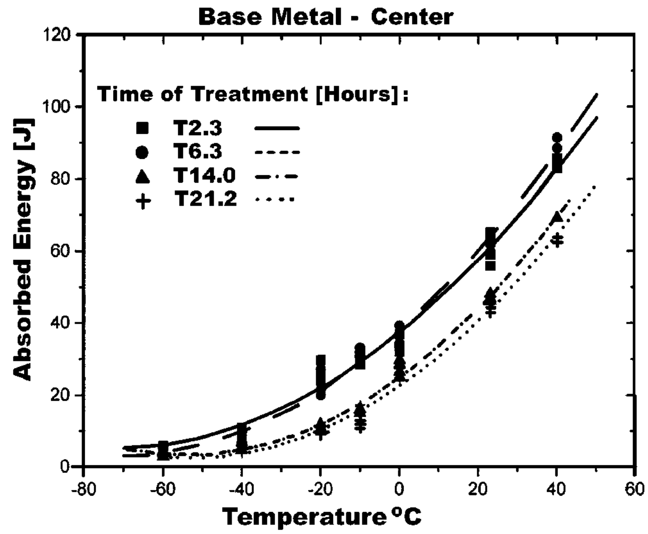

Fig. 16 Charpy absorbed impact energy of the BM (region of half-thickness), for the different heat treatments, as a function of the testing temperatures

the BM and HAZ decreased slightly with the time of heat treatment, whereas there was a small increase of the elongation (EL) and area reduction (AR) with the time of treatment. Fracture always occurred outside the weld.

4.4 Hardness Measurements

Hardness measurements were made on the BM and HAZ. The measurements were made at 5 mm from the plate surface and at half-thickness of the plate and along the HAZ, in the flat side of the K joint.

Table 4 shows the Rockwell-A and Vickers hardness values for each treatment. It shows that there is a decrease of hardness with the holding time at 620 °C.

4.5 Charpy-V-Notch Impact Testing

The results of the Charpy impact tests of the heat-treated material are shown in Fig. 15 to 18, where the absorbed energies are plotted as a function of the testing temperatures, for the different heat treatments.

From the figures, it is possible to see that the HAZ always presented higher impact resistance and lower transition temperature than the BM, for all heat treatments. The impact energy decreased for the heat treatments longer than 6.3 h, with the BM presenting a more pronounced decrease. Testpieces taken from the surface of the plate always presented higher impact energies than the ones from the center, for all treatments.

Figure 19 and 20 show the values of mean absorbed impact energy at the surface and at half-thickness of the BM as a function of the time of heat treatment, for the different testing temperatures.

Figure 21 and 22 show those values for the HAZ, at the same positions, also as a function of the time of heat treatment, for the different testing temperatures.

A reference line corresponding to a ductile-brittle transition temperature of 20 J is also drawn in the figures.

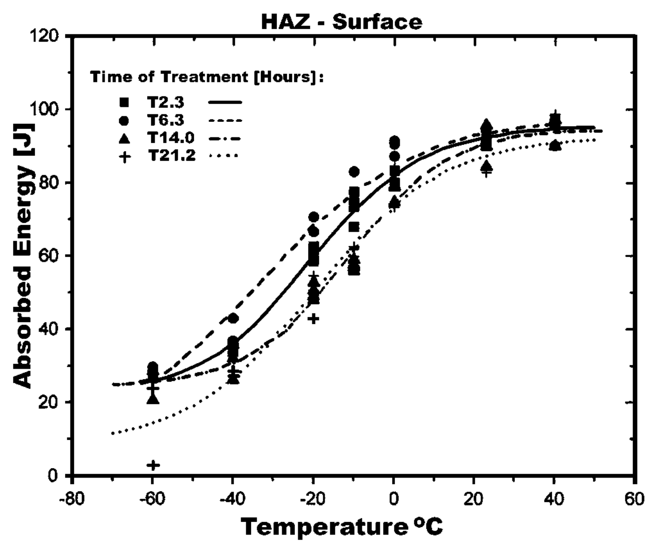

Fig. 17 Charpy absorbed impact energy of the HAZ (region of the surface), for the different heat treatments, as a function of the testing temperatures

The figures show that, for the majority of the testing temperatures, the impact resistance increases slightly until 6.3 h of heat treatment and then decreases. For the HAZ, for treatments until 10 h, the transition temperature remained at about −60 °C. For larger times, the transition temperature increased until attaining, after 21.2 h of treatment, a transition temperature of about −50 °C. The transition temperature of the BM changed from −20 °C, for treatments until 7.3 h, to −5 °C, for the treatment of 21.2 h.

4.6 CTOD Testing

The results of the CTOD tests are shown in Table 5, where the mean values of CTOD at maximum load are presented as

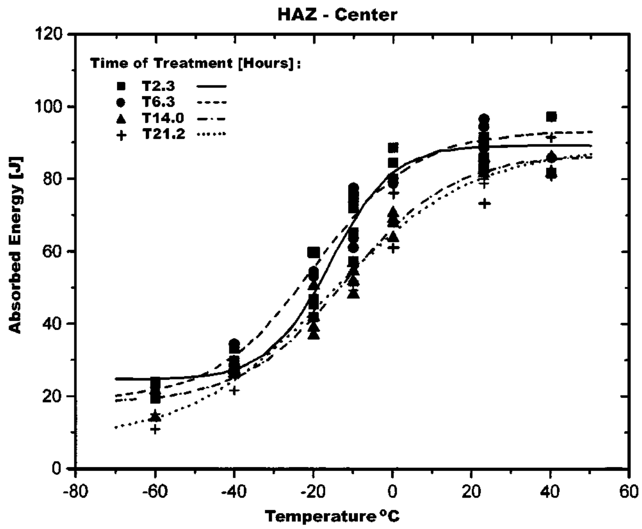

Fig. 18 Charpy absorbed impact energy of the HAZ (region of half-thickness), for the different heat treatments, as a function of the testing temperatures

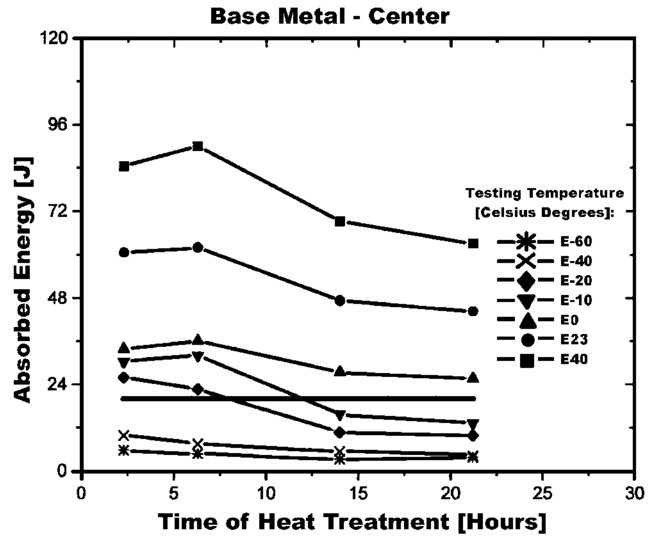

Fig. 20 Charpy absorbed impact energy of the BM (region of half-thickness), for the different testing temperatures, as a function of the time of treatment at 620 °C

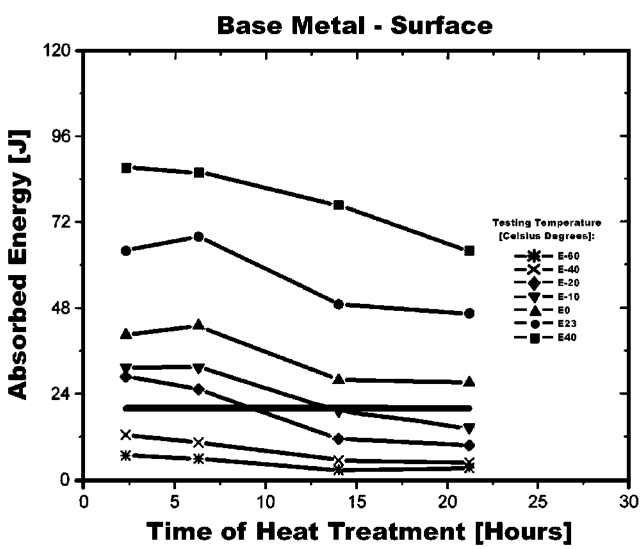

Fig. 19 Charpy absorbed impact energy of the BM (region of the surface), for the different testing temperatures, as a function of the time of treatment at 620 °C

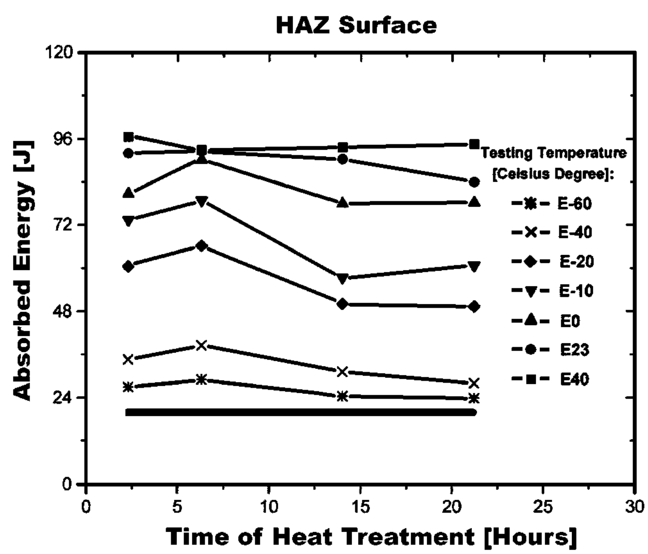

Fig. 21 Charpy absorbed impact energy of the HAZ (region of the surface), for the different testing temperatures, as a function of the time of treatment at 620 °C

Table 4 Hardness values for the different heat treatments

	Time of Heat Treatment (h)							
Region	**2.3**		**6.3**		**14.0**		**21.2**	
Hardness	RAHN	VHN	RAHN	VHN	RAHN	VHN	RAHN	VHN
Surface	46	153	45.5	150	45	140	44	139
Half-thickness	45	149	45	148	44	140	42.5	137
HAZ	51	165	51	164	48.5	157	48	150

RAHN—Rockwell A hardness number
VHN—Vickers hardness number

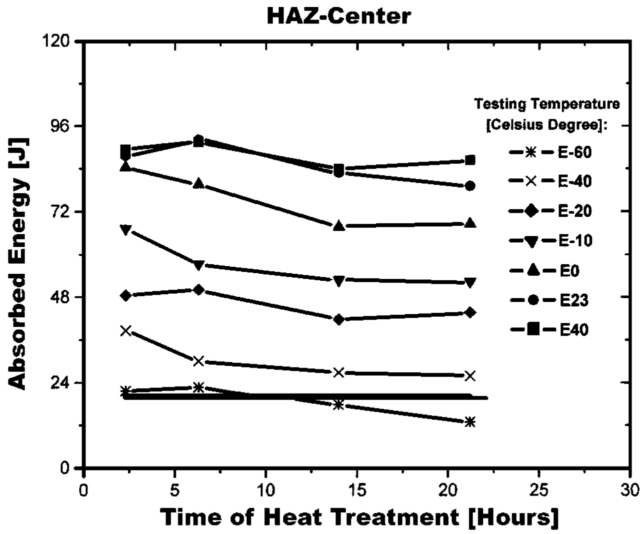

Fig. 22 Charpy absorbed impact energy of the HAZ (region of half-thickness), for the different testing temperatures, as a function of the time of treatment at 620 °C

a function of the testing temperatures. From the results, it is possible to draw the following observations:

a. Base Metal. The values of CTOD obtained for the treatments of 2.3 and 6.3 h are similar, with the CTOD values decreasing at temperatures lower than −30 °C. For the treatment of 21.2 h, the CTOD values start to decrease markedly below 0 °C. At the lower temperatures, below −40 °C, the CTOD values are similar for all treatments.

b. Heat-Affected Zone. A behavior similar to that of the BM can be observed when the CTOD values are compared for the treatments of 2.3 and 6.3 h, although the decrease of toughness started to occur from −50 °C on. For the treatment of 21.2 h, CTOD started to drop at −40 °C. At the lowest testing temperatures, the obtained values of CTOD were similar. The values of CTOD obtained in the temperatures where there was a drop in toughness are associated with the occurrence of pop-ins.

5. Discussion

5.1 Tensile Properties

The obtained results showed that the YL, UTS, and hardness decreased slightly with the time of heat treatment. The variation of strength between the treatments of 2.30 and 21.20 h was about 8%. On the other hand, the EL and AR had a slight increase with the time of treatment.

The standard ASTM A516 G70 specifies the following values for the mechanical properties:

- YL: minimum of 280 MPa,
- UTS: 485 to 620 MPa, and
- EL: minimum of 21%.

The comparison of the required and obtained values indicates that, for the heat treatment of 21.20 h, the UTS of the material fell below the required level both for the BM and the HAZ at the surface and the center of the plate. The same happened with the YL at the center of the plate. A similar result was obtained by Komkol[12] when studying different steels used in the construction of spheres and pressure vessels.

One of the reasons for the fall of the strength of the BM was the spheroidization and coarsening of the pearlite, whereas, in the HAZ, it was attributed to the spheroidization of the carbides.

Other researchers[13–15] also observed a similar behavior when analyzing the effect of the time and temperature of the stress relief heat treatment on the mechanical properties and fracture toughness. Besides the metallurgical changes pointed out above, other changes can take place such as the impinging of dislocations and overaging, which can affect the tensile properties, depending on the chemical composition and welding procedure adopted.

The comparison of the mechanical properties obtained at the surface and center of the plate shows that the surface presented a slightly higher strength and hardness. In the case of the BM, this is due to a finer microstructure in this region,[16–19] whereas, in the HAZ, this behavior may result from a smaller number of thermal cycles imposed by the multiple welding passes, resulting in less tempering in this region.[20–22]

5.2 Impact Testing

The results obtained from the impact tests allow the following observations:

- for a given temperature, the impact resistance decreased with the increase of time of treatment, for treatments longer than 6.3 h;
- the impact resistance was larger at the surface than at the center of the plate;
- the HAZ showed a larger impact resistance than the BM; and
- the ductile-brittle transition temperature increased with the time of heat treatment.

The factors that affect the impact resistance of the welded joints of pressure vessel steels have been subjected to several studies.[14,21,23,24] The effect of the grain size and impurity level on the fracture resistance was studied by Doubby[25] and Fairchild.[15] They observed a higher fracture toughness and smaller transition temperature in steels with a finer microstructure and a small impurity content. This type of behavior is also observed when the microstructure and impurity content of the surface and center of the plate are compared. The central region has a coarser microstructure and more impurities,[17,18] presenting, as a consequence, lower toughness.

The fracture resistance of the HAZ is a function of the chemical composition and microstructure of the steel and of the thermal cycle imposed.[20,21,26,27] Multipass weldings with adequate parameters, temperature control of the preheating and interpasses, and postweld heat treatments are the basic conditions to obtain an adequate fracture toughness. When these conditions are met, the final microstructure contains a large fraction of fine-grained acicular ferrite.

The observation of the HAZ of the present work showed

Table 5 CTOD values of the BM and HAZ for the different heat treatment imes

Temperature (°C)	CTOD values (mm)					
	Time of heat treatment (h)					
	2.3		6.3		21.2	
	BM	HAZ	BM	HAZ	BM	HAZ
27	0.998	0.872	0.997	0.937	0.926	0.855
	0.968	0.802	0.911	0.912	0.919	0.955
0	0.990	0.980	1.074	0.895	0.933	0.962
	0.970	0.863	1.013	0.778	0.903	0.982
−20	0.907	0.815	1.031	0.869	0.433	0.890
	0.907	0.710	0.841	0.853	0.397	0.890
−30	0.943	…	0.920	…	0.353(a)	0.725
	0.800	…	…	…	0.329	…
	0.570	…	…	…	0.220	0.835
−40	0.372(a)	0.870	0.308(a)	0.495	0.232(a)	0.537(a)
	0.199	0.910	0.219	0.942	0.124	0.393
	0.278	…	…	0.845	0.179	0.328
−50	…	0.780	…	…	…	…
	…	0.970	…	…	…	…
−60	0.110(a)	0.380(a)	0.120(a)	0.253(a)	0.117(a)	0.217(a)
	0.121	0.242	0.131	0.210	0.092	0.276
	0.152	0.374	…	0.257	0.110	…

(a) Occurrence of pop-in

that its microstructure is formed of acicular ferrite and plates of aligned carbides (Fig. 9).

The postweld heat treatment is commonly used for reducing the residual stresses in the welded joints of spheres and pressure vessels. This treatment improves the fracture resistance due to the simple fact that it promotes an increase in the critical acceptable defect size at a given stress level.[24] Another beneficial effect of the heat treatment is the improvement of toughness resulting from the tempering of the microstructure,[19,20] although there are cases of fracture toughness reduction due to the heat treatments.[27,28]

There are various possible ways of obtaining the ductile-brittle transition temperature. In the present work, the transition temperature was chosen as that corresponding to an absorbed fracture energy of 20 J, which is the value specified by the ASME code for the lower design temperature. Figures 19 to 22 show the mean absorbed energies at fracture, for each testing temperature, as a function of the time of heat treatment. A line corresponding to a fracture energy of 20 J was also drawn in the figures. The observation of the figures motivate the following observations:

- the transition temperature increases with the time of heat treatment, with the BM presenting a larger increase; and
- the HAZ presents a lower transition temperature for all heat treatments.

Similar results were obtained by Konkol,[12] who showed that the increase in the transition temperature was due to microstructural changes in the material resulting from the heat treatments. The observation on the optical microscope showed a progressive spheroidization of the carbides with the time of heat treatment for all steels of his study. However, there are some other possible causes for the changes in fracture toughness, depending on the chemical composition and microstructure of the steel, such as tempering, temper embrittlement, transformation of retained austenite, elimination of strain hardening, and precipitation hardening.

The decrease of fracture toughness due to the coarsening and spheroidization of the pearlite was also observed by Fairchild[15] when studying the influence of temperature on the stress relief heat treatment. Using instrumented Charpy tests, he observed that there was an increase in the transition temperature with the temperature of the treatment due to the coarsening and spheroidization of the pearlite. Figures 7 and 8 of the present work show that there was a substantial spheroidization of the carbides with the treatment of 21.2 h when compared to the treatment of 2.3 h.

Another important observation is that the carbides in the BM are not fully spheroidized, presenting regions still with a pearlitic morphology. This is related to the impact behavior of the BM, which presents an increase of transition temperature with the time of treatment. On the other hand, the HAZ showed only a small variation of the transition temperature with the increase of the time of treatment.

The validity of the criterion adopted for the transition temperature of a fracture energy of 20 J is corroborated by the morphology of the fracture surfaces of the Charpy testpieces, which was cleavage for this absorbed energy, as shown by Fig. 23 and 24, for both BM and HAZ.

5.2 CTOD Testing

The results of the CTOD tests showed that there was a decrease of toughness with the increase of time of treatment for times greater than 6.3 h. For the tests at low temperature, the fracture toughness of the HAZ was higher than that of the BM.

Fig. 23 Cleavage fracture morphology of a Charpy testpiece of the BM with an absorbed fracture energy of 20 J

Fig. 24 Cleavage fracture morphology of a Charpy testpiece of the HAZ with an absorbed fracture energy of 20 J

Threadgill[14] studied the effect of the time of stress relief heat treatment for a carbon-manganese steel with additions of niobium and aluminum, using Charpy and CTOD tests. The results of the Charpy tests showed that, for times of treatment to 4 h, there was a small increase in the transition temperature, whereas the results of the CTOD tests showed that there was a tendency for an increase in the transition temperature with the time of treatment, with lower values of CTOD being associated with the occurrence of pop-ins for the treatments at larger times.

The comparison of the results obtained with the Charpy and CTOD tests in the present work shows that in both cases there was an increase in the transition temperature and a decrease in fracture toughness for the treatments at the larger times at the temperature of 620 °C.

As the fracture toughness for the treatments of 2.30 and 6.30 h were similar, the main reason for the decrease in toughness for the treatments for larger times was the spheroidization of the carbides. The decrease in hardness and mechanical strength with the time of heat treatment corroborates this fact.

Although there was a decrease in toughness for the treatments at larger times, the steel still presented a good fracture toughness, principally the HAZ, as shown by the high values of CTOD.

6. Conclusions

The effect of postweld heat treatments at 620 °C for different periods of time on the hardness values, tensile properties, Charpy impact resistance, and CTOD values of an ASTM A 516 G 70 pressure vessel steel were evaluated. The results obtained led to the following conclusions.

- There was a small decrease in hardness and in mechanical strength with the increase in the time of heat treatment.
- The fracture toughness decreased for heat treatments longer than 6.3 h.
- The ductile-brittle transition temperature increased with the increase of the time of heat treatment.
- The deterioration of the mechanical strength and fracture toughness with the time of heat treatment is due to microstructural changes taking place in the material, mainly spheroidization of the pearlite of the BM and coarsening of the carbides in the HAZ.
- Smaller grain sizes and impurity content produce higher fracture toughness, even for the more prolonged heat treatments.
- For the welding procedure adopted, the fracture toughness of the HAZ was superior to that of the BM.
- Even for the most prolonged heat treatments, to 21.2 h, the obtained values of CTOD were kept at acceptable levels, mainly in the HAZ.
- There was a good correlation between the results of the Charpy and CTOD tests.

Acknowledgments

The financial support from CAPES and CNPq is gratefully acknowledged. The authors thank J.C.G. Teixeira for his helpful comments.

References

1. J.E. Cantwell: *Corrosion* 88, St. Louis, MO, 1988, paper no. 157.
2. *ASME Boiler and Pressure Vessel Code*, Section VIII, Divisions 1 and 2, ASME, Fairfield, NJ.
3. *Standard Specification for Pressure Vessel Plates, Carbon Steel for Moderate and Lower Temperature Service*, ASTM A 516, ASTM, Philadelphia, PA.
4. *AWS D.1.1-81*, 5th ed., American National Standards Institute, New York, NY, 1981.
5. *Standard Test Methods for Tension Testing of Metallic Materials [Metric]*, ASTM E 8M, ASTM, Philadelphia, PA, 1989.
6. *Standard Methods for Rockwell Hardness and Rockwell Superficial Hardness of Metallic Materials*, ASTM E 18, ASTM, Philadelphia, PA, 1989.
7. *Standard Methods for Microhardness of Materials*, ASTM E-384, ASTM, Philadelphia, PA, 1984.
8. *Standard Methods for Notched Bar Impact Testing of Metallic Materials*, ASTM E 23, ASTM, Philadelphia, PA, 1980.
9. *Standard Terminology Relating to Fracture Testing*, ASTM E 616, Philadelphia, PA, 1982.
10. *Methods for Crack Opening Displacement (COD) Testing*, BS 5762/79, BSI, London, UK, 1979.
11. H.G. Squirrell: *Recommended Procedures for the Crack Opening Displacement (CTOD) Testing of Weldments*, Welding Institute Research, Cambridge, UK, 1986, No. 31.

12. P.J. Konkol: *Effect of Long-Time Post Weld Heat Treatment on the Properties of Constructional Steel Weldements*, Welding Research Council, No. 330.
13. R.D. Stout: *Postweld Heat Treatment of Pressure Vessels*, Welding Research Council, New York, NY, 1985, No. 305.
14. P.L. Threadgill: Welding Research Report No.253, Welding Research Council, New York, NY, 1984.
15. D.P. Fairchild: *The Effects of Post Weld Heat Treatment on the Microstructure and Toughness of Offshore Platform Steels*, Exxon Production Research Company.
16. C. Bonnet: *Soudage Tech Connexes*, 1980, July–Aug., pp. 209-27.
17. A.M. Pope: "Brittle Fracture in Welded Joints," Internal Report, Petrobras, Rio de Janeiro, Brazil (in Portuguese).
18. *Metals Handbook*, 9th ed., ASM, Metals Park, OH, 1978, vol. 1.
19. G.R.Wang: *Microalloying Additions and HAZ Fracture Toughness in HSLA Steels*, Welding Research Supplement, Welding Research Council, New York, NY, 1990, pp. 14-22.
20. R.E. Doubly: *HAZ Toughness of Structural and Pressure Vessel Steels—Improvement and Prediction*, Welding Research Council, New York, NY, Aug. 1979, pp. 225-37.
21. C. Thaulow, A.J. Paauw, A. Gunleiksrud, and O.J. Naess: *Metal Construction*, vol. 17, No. 2, February 1985, pp. 94-99.
22. R. Farrar: *Metal Constr.*, 1987, vol. 19 (17), pp. 392-97.
23. G.M. Evans: *Welding J.*, 1986, pp. 3265-3345.
24. R.E. Douby: Welding Institute Report No. 14, Welding Research Council, New York, NY, 1976.
25. H. Toskoaki: Nippon Steel Technical Report No. 36, Nippon Steel, Jan. 1988.
26. K. Uchino: *Development of 50kgf/mm^2 Class Steel for Offshore Structural Use with Superior HAZ Critical CTOD*, Welding Institute Research, Cambridge, UK, 1980.
27. K.E. Dorschu: Welding Research Report Bulletin No. 231, Welding Research Council, New York, USA.
28. R.A. Swift: *Welding J.*, 1971, vol. 50 (8).